ELSEVIER

Journal of Organometallic Chemistry 646 (2002) 179–190

Journal of Organometallic Chemistry

www.elsevier.com/locate/jorganchem

Regio- and stereoselective addition of sterically hindered silylboranes to terminal alkynes

José Carlos Araujo Da Silva [a], Marc Birot [a,*], Jean-Paul Pillot [a,*], Michel Pétraud [b]

[a] *Laboratoire de Chimie Organique et Organométallique, UMR 5802 CNRS-UB 1, Université Bordeaux 1, 351 cours de la Libération, F-33405 Talence Cedex, France*

[b] *CESAMO, Université Bordeaux 1, 351 cours de la Libération, F-33405 Talence Cedex, France*

Received 11 July 2001; accepted 26 September 2001

Abstract

Novel stable organosilylboranes possessing dimesityl groups attached to boron were synthesised. They gave an addition reaction with terminal acetylenic hydrocarbons in the presence of a transition metal complex. Thus, (diphenylmethylsilyl)dimesitylborane and (diphenyl-*tert*-butylsilyl)dimesitylborane reacted in good yields with phenylacetylene and alk-1-ynes in the presence of $Pd_2(dba)_3(etpo)_2$ as a catalyst. The structures of the products were determined by NMR spectroscopy using INEPT techniques coupled to computational simulation. Various heteronuclear coupling constants $J_{^{13}C-H}$ and $J_{^{29}Si-H}$ were determined for the first time in this series. The results showed that the dimesitylboryl group added to the terminal acetylenic carbon atom and the organosilyl group to the internal carbon atom, according to a regio- and stereoselective *syn*-addition.

Keywords: Organosilylboranes; Silaboration; Palladium catalyst; ^{13}C- and ^{29}Si-NMR; Heteronuclear coupling constants; Stereochemistry

1. Introduction

The first stable organosilylboranes were reported about 40 years ago [1–3]. This puzzling class of compounds contains a σ-bond between a tetravalent silicon and a trivalent boron atom. Apart from the pioneering work of Nöth et al. and scarce subsequent reports in the literature, compounds possessing $Si–B^{III}$ bonds have only focused very little attention over the last decades [4–8]. Conversely, organosilicon chemistry has been receiving an explosive development during the same time. Because silicon possesses a marked electropositive character and boron is an electron-deficient heteroatom, compounds containing $Si–B^{III}$ bonds are not very stable. Generally, silylboranes are difficult to synthesise and there are only few different structural edifices accessible, more particularly when boron is bound to alkyl substituents. Classical routes using organometallic condensations lead to borates, i.e. compounds possessing tetracoordinated boron atoms. But organosilylboranes are more stable when boron bears electronegative heteroatoms such as oxygen and nitrogen, and some authors have emphasised that the Si–B bond was then unexpectedly chemically inert [7]. The recent discovery that compounds containing Si–B bonds possess many interesting properties has focused renewed interest in this series. Thus, Ito and co-workers have reported that organosilylboranes possessing electronegative substituents on boron added regio- and stereospecifically to ethylenic and acetylenic substrates, in the presence of platinum or palladium complexes as catalysts [9–12]. Tanaka and co-workers has subsequently reported that a similar silaboration of alkynes and silaborative diyne cyclisation were promoted by a palladium catalyst with an etpo ligand [13]. The former authors have extended this reaction to 1,2-dienes and methylene cyclopropanes, using various transition metal-based catalysts [14,15]. Recently, we have reported preliminary results on the synthesis and UV–vis properties of a new class of aromatic silylboranes stabilised by mesityl groups attached to boron instead of electronegative heteroatoms [16,17]. Availability of data on this new series was significant to gain a better knowledge of the properties of the Si–B bond. Moreover, it was interesting to compare the chemical reactiv-

* Corresponding authors.

0022-328X/02/$ - see front matter
PII: S0022-328X(01)01339-0

ity of these new compounds with that of previously described silylboranes. We report on the addition of these organosilylboranes to acetylenic hydrocarbons in the presence of a palladium catalyst. The structures of the addition products were investigated by NMR spectroscopy (^{1}H, ^{13}C and ^{29}Si) using INEPT 1D and 2D sequences complemented by computational line-shape simulations.

2. Results and discussion

2.1. Synthesis of sterically hindered organosilylboranes

Novel organosilylboranes possessing bulky dimesityl groups attached to boron were synthesised in good yields according to our previously reported route by using a modified experimental procedure (compounds **1** and **2**, Eq. (1)) [17].

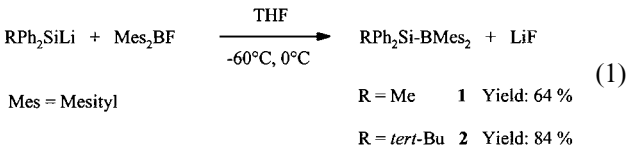

(1)

Compounds **1** and **2** are powders that can be handled in air for short times. They are reasonably stable but slowly oxidise over several days. They melt before decomposition and are kept unchanged for weeks under inert atmosphere at room temperature. Their ^{29}Si-NMR spectra exhibited chemical shifts in roughly the same range as their disilane homologues (-25.0 and -20.1 ppm for **1** and **2**, respectively). Conversely, boron nuclei are deshielded in ^{11}B-NMR spectroscopy (110 and 103 ppm for **1** and **2**, respectively) with respect to organosilylboranes bearing heteroelements linked to boron, e.g. $\delta = 34.3$ ppm for the boron nucleus in the case of compound **4** (Scheme 1) [8]. But the ^{11}B-NMR chemical shifts are in the same range as those previously reported for related diboranes [18].

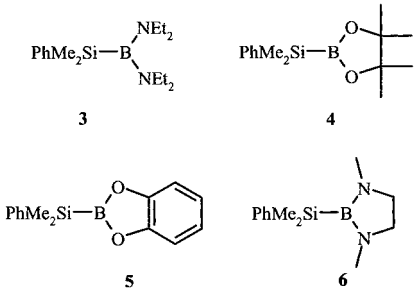

Scheme 1. Organosilylboranes stabilised by electronegative groups.

2.2. Addition of silylboranes **1** and **2** to alk-1-ynes

Ito et al. have found that silylboranes **3**–**6** containing oxygen or nitrogen atoms (Scheme 1), react with carbon–carbon triple bonds in the presence of platinum- or palladium-based catalysts, according to a regioselective *syn*-addition mechanism.

They have shown that the boryl group added to the terminal carbon atom in the case of terminal acetylenic derivatives. Moreover, they have investigated a wide range of transition metal complexes, showing that palladium–isonitrile complexes were amongst the most efficient catalysts [11,12]. On the other hand, Wilkinson's catalyst was totally inactive, although it can be efficient in other reactions involving boron, such as hydroboration reactions. In the case of terminal olefins, the Si–B bond added in a reverse way, the boryl group being linked to the internal carbon atom. In the same way, Tanaka et al. have reported that $Pd_2(dba)_3(etpo)_2$ [etpo = $P(OCH_2)_3CEt$] is an effective catalyst for the stereoselective addition of **6** to oct-1-yne (92% yields) and that the addition of borostannanes under the same conditions led to similar results [19].

We have shown that sterically hindered silylboranes **1** and **2** added to the triple bond of terminal alkynes in the presence of $Pd_2(dba)_3(etpo)_2$ as the catalyst (Eq. (2)).

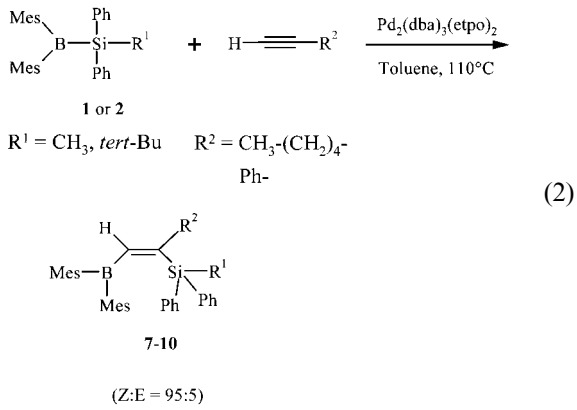

(2)

Compound **1** and hept-1-yne ($R^2 = C_5H_{11}$–) in slight excess were heated at 120 °C for 12 h in toluene as the solvent, in the presence of the catalyst. The IR spectrum of product **8** revealed that the absorption bands of the starting acetylenic compounds at 2130 cm^{-1} ($\nu_{C\equiv C}$) and 3340 cm^{-1} ($\nu_{C-H_{acetylenic}}$) disappeared. Interestingly, the ^{29}Si- and ^{11}B-NMR chemical shifts appeared around -13 and 80 ppm, respectively, whereas no signal corresponding to unreacted silylborane remained. Similarly, the reaction was performed with silylborane **2** and phenylacetylene. The results are shown in Table 1.

Thin-layer chromatography (TLC), ^{1}H- and ^{13}C-NMR showed that one major isomer was formed in each case. Integration of the ethylenic protons of the

Table 1
Addition products of organosilylboranes to terminal acetylenic hydrocarbons

R^1	R^2	Product	Z:E	Overall yield (%)
Me	Ph	**7**	95:5	67
Me	$CH_3(CH_2)_4$–	**8**	95:5	65
tert-Bu	Ph	**9**	95:5	55
tert-Bu	$CH_3(CH_2)_4$–	**10**	95:5	60

crude reaction mixtures was not possible, because of the presence of signals of dba in the same region. So the products were first purified by liquid chromatography. Owing to the results reported previously in the literature [8,13], the products were assumed to be the Z/E isomers resulting from the addition of the dimesitylboryl group to the terminal acetylenic carbon.

Reaction of oct-1-yne with silylborane **2** under the same conditions gave similar results, but attempts to perform addition of silylboranes **1** and **2** to internal acetylenic hydrocarbons and various ethylenic substrates under similar conditions were unsuccessful. Other catalysts such as the platinum-based catalysts used by Ito et al., as well as Cp_2TiMe_2 and Cp_2ZrMe_2, led to the consumption of the silylboranes but did not give the expected silaboration products.

2.3. NMR studies

Ito and co-workers have inferred the regio- and stereochemistry of the addition of silylboranes to unsaturated substrates from the observation of NOE effects in a few examples [14,15]. To show direct evidence of the structure of the silaboration protons, we turned to ^{13}C- and ^{29}Si-NMR spectroscopies to measure the various heteronuclear coupling constants thanks to the INEPT technique.

2.3.1. Regiochemistry of the silaboration

2.3.1.1. Addition of (diphenylmethylsilyl)dimesitylborane to hept-1-yne. In a first approach, the regioselectivity of the reaction was inferred from ^1H- and ^{13}C-NMR spectroscopies. Besides the expected signals corresponding to the different aliphatic and aromatic protons, the ^1H-NMR spectrum of **8** exhibited a low field singlet at 7.6 ppm (1H) assigned to the ethylenic H. Moreover, the proton-decoupled ^{13}C-NMR spectrum of this product showed two deshielded signals at 156 and 157 ppm. A 2D ^1H–^{13}C-NMR correlation (HMQC) corroborated that only the more deshielded carbon nucleus at 157 ppm was coupled with the proton at 7.6 ppm. This signal was assigned to the ethylenic carbon bearing both the dimesitylboryl group and the ethylenic proton. Therefore, the boron atom added to the terminal ethylenic carbon. These results were also supported by the strong deshielding effect of the $BMes_2$ group previously reported for other substrates [20,21].

2.3.1.2. Addition of (diphenylmethylsilyl)dimesitylborane to phenylacetylene. One of the four possible isomers **7a**–**d** might be expected as the major product from the addition of **1** to the triple bond of phenylacetylene (Scheme 2). Assuming that a long-distance coupling constant through the ethylenic bond should be very weak and consequently not observed (i.e. $^4J_{^{13}C_5-^1H}$), the ^{13}C-NMR INEPT spectra of the carbon nucleus of the methyl group bounded to the silicon atom (C_5) should exhibit quite different patterns depending on the regiochemistry of the reaction, as shown in Scheme 2 (spectra **A** or **B**).

The experimental ^{13}C-NMR spectrum of C_5, centred at -0.7 ppm, was obtained by using a non-decoupled INEPT sequence (Fig. 1).

This spectrum was consistent with structures **7a** or **7b**, since it exhibited only four lines. If stereoisomers **7c** or **7d** were formed, the corresponding ^{13}C-NMR spectrum should exhibit eight lines resulting from the coupling with the three neighbouring H ($^1J_{^{13}C-^1H}$) and the ethylenic H ($^3J_{^{13}C_5-^1H} = 0.3–1.6$ Hz [22]) (spectrum **B**). However, very weak additional peaks were observed in the same region, which probably corresponded to the other isomers in very small proportions. Similar results were obtained concerning the regiochemistry of the addition of **1** to hept-1-yne, corroborating that the dimesitylboryl group added to the terminal acetylenic carbon.

2.3.1.3. Addition of (diphenyl-tert-butylsilyl)dimesitylborane to hept-1-yne. The four plausible silaboration products are shown in Scheme 3 (**10a**–**d**).

The non-decoupled ^{13}C-NMR INEPT spectrum of the addition product was obtained under the same conditions as in the previous case. Fig. 2 displays the region of the aliphatic carbons, namely the Me groups and the quaternary carbon of the *tert*-butyl group linked to silicon (C_5).

If regioisomers **10a** or **10b** were formed, no long-distance coupling between C_5 and the ethylenic H should be observed (i.e. $^4J_{^{13}C-^1H}$). Therefore, only $^2J_{^{13}C_5-^1H}$ coupling constants between C_5 and nine neighbouring H of the *tert*-butyl group were expected. Conversely, if reverse addition products were formed (compounds **10c** or **10d**), a $^3J_{^{13}C-^1H}$ coupling constant between C_5 and the ethylenic H should be observed. Because a tangled up spectrum was obtained in this region, no coupling constant involving C_5 could be drawn out. This is due to the weak response of this nucleus and to the fact that its spectrum overlapped the signals of the CH_3 of the mesityl groups ($^1J_{^{13}C-^1H} = 128$ Hz).

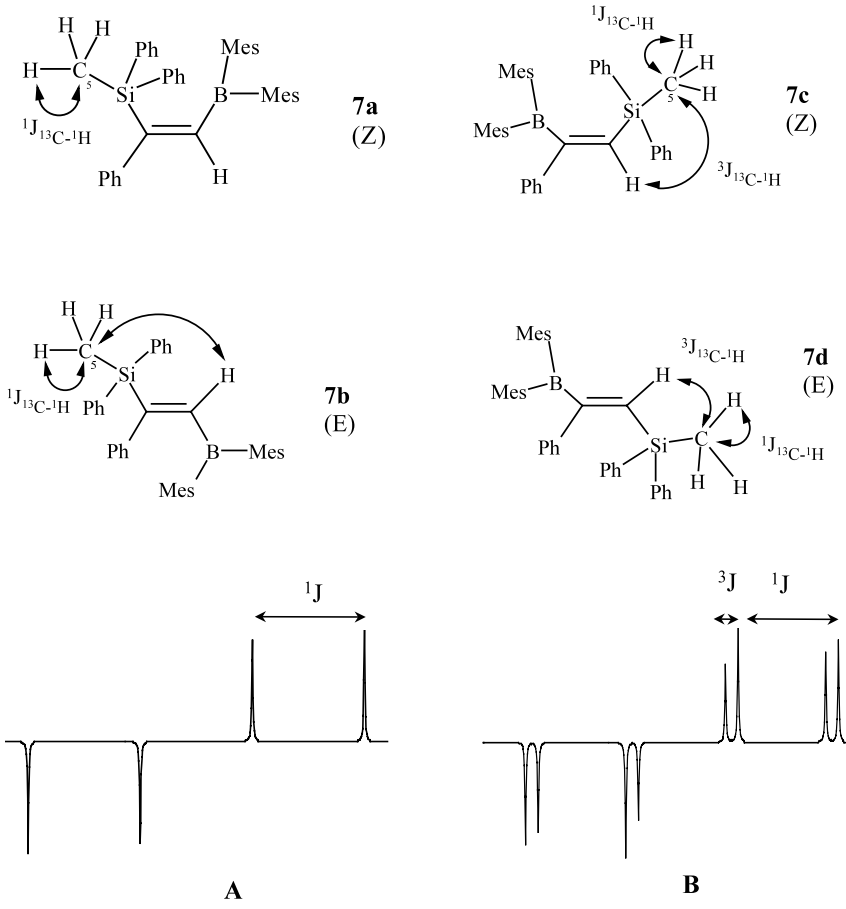

Scheme 2. Expected $J_{^{13}C-{}^1H}$ coupling for C_5 related to Z/E isomers **7a**–**d** and corresponding ^{13}C-NMR INEPT theoretical spectra.

We reasoned that the use of 2D INEPT BIRD *J*-resolved ^{13}C-NMR sequences to observe the aliphatic carbons should help us overcome this difficulty for the following reasons [23,24]. (i) The phases of the signals depend on the signs of the coupling constants and the systems of spins, for a given value of the polarisation delay τ. (ii) The observed carbon atoms are coupled at the first order. This feature takes advantage of an enhanced sensibility resulting from the most efficient polarisation transfer. (iii) The phases of the BIRD

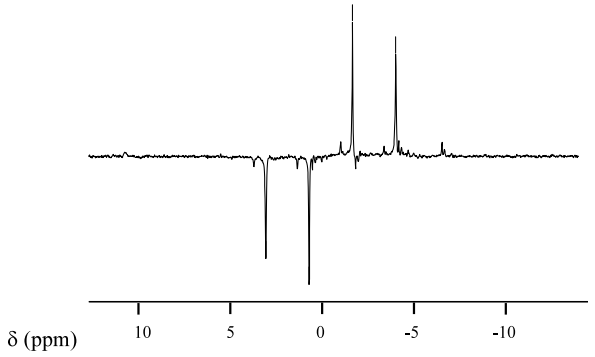

Fig. 1. Experimental ^{13}C-NMR INEPT spectrum of C_5 in product **7**.

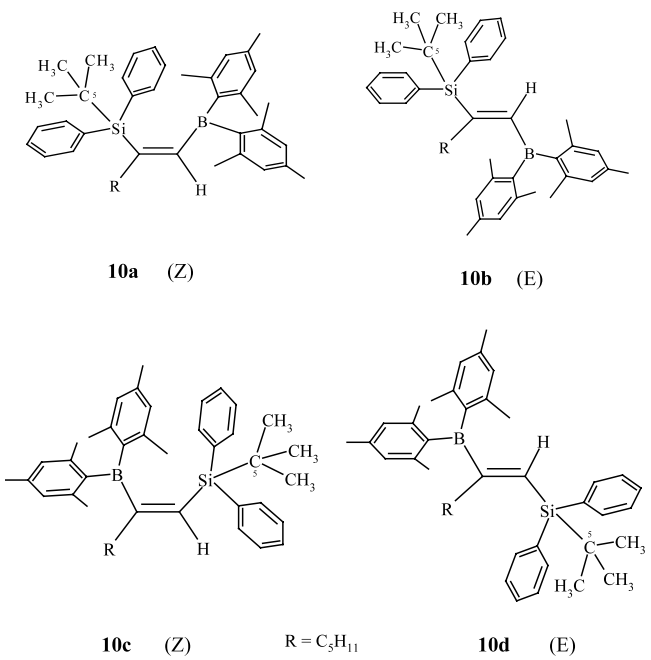

Scheme 3. Possible isomers **10a**–**d** for the silaboration of hept-1-yne by (diphenyl-*tert*-butylsilyl)dimesitylborane (**2**).

pulses can be chosen in a way to selectively mask any undesirable $^{n}J_{^{13}C-^{1}H}$ coupling constants.

In our case, the BIRD pulses were chosen to eliminate the coupling constant $^{1}J_{^{13}C-^{1}H}$ ($\sim$128 Hz) of each Me group. The chart giving the response of the different carbon nuclei is shown in Fig. 3.

Individual ^{13}C INEPT spectra can be easily picked up from this chart. On the other hand, the SIMEPT program enabled us to calculate the theoretical INEPT spectrum of a nucleus X from a set of parameters (polarisation delay τ, refocusing delay Δ, coupling constants J_{X-H} and J_{H-H}) [25].

Thus, the experimental and simulated spectra of the quaternary carbon atom C_5 in product **10** are displayed in Fig. 4.

The simulation was achieved by varying J, whereas τ, Δ and the half-height width were fixed by the experiment. A good agreement between the simulated and experimental spectra was obtained for a $J_{^{13}C-^{1}H}$ value of -3.3 Hz (9H). As the phase of the signal was

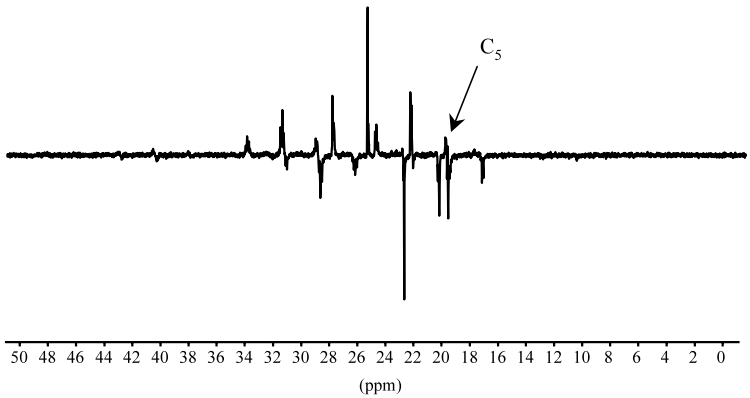

Fig. 2. Non-decoupled ^{13}C-NMR INEPT spectrum of product **10**.

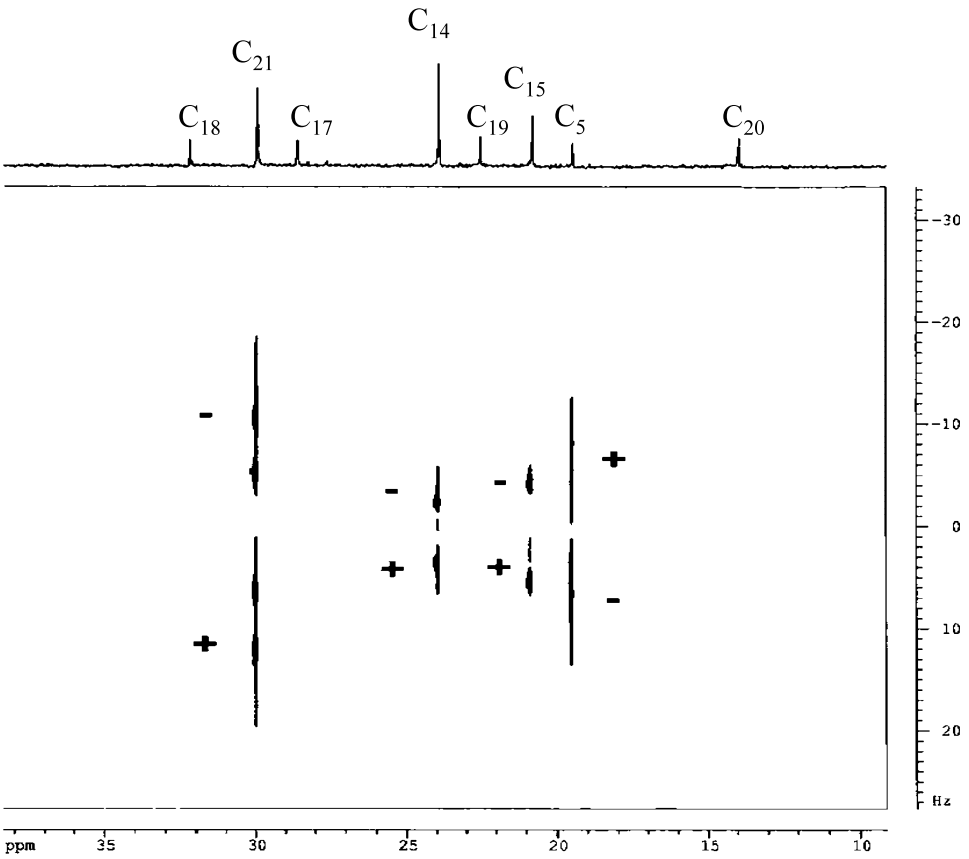

Fig. 3. ^{13}C-NMR 2D INEPT BIRD J-resolved chart of the Me and C_5 carbon atoms in product **10**.

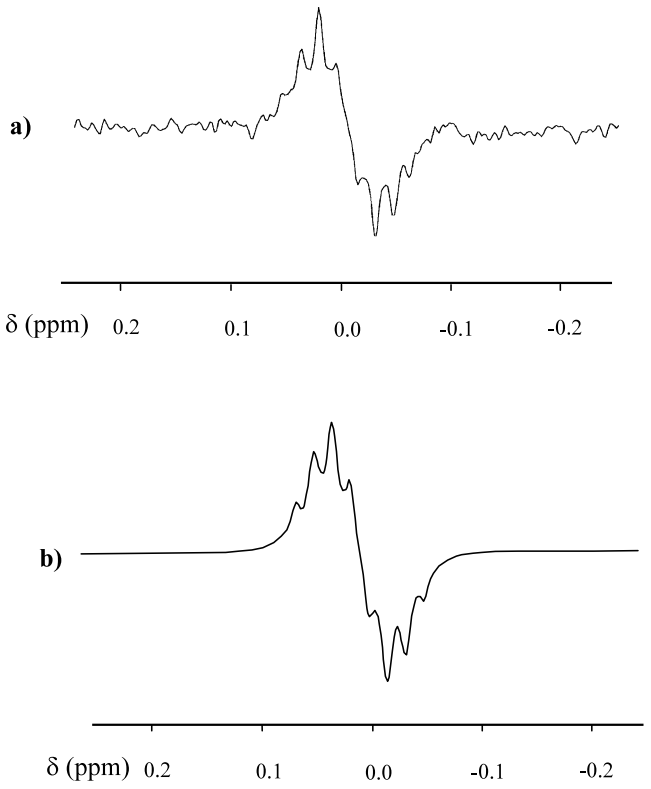

Fig. 4. (a) Section of the chart in Fig. 3 corresponding to C_5. (b) Simulated spectrum.

opposite to that of the methyl groups (where only $^3J_{^{13}C-^1H}$ could be observed), we can conclude that C_5 was coupled with its nine neighbouring H (i.e. $^2J_{^{13}C-^1H} = -3.3$ Hz) only. No $^3J_{^{13}C-^1H}$ or $^4J_{^{13}C-^1H}$ constant could be found out. This achievement led us to unambiguously assign the product the structures **10a** or **10b**, with silicon at the internal position of the double bond and the dimesitylboryl group at the terminal carbon.

2.3.2. Stereochemistry

Evidence of the stereochemistry of the silaboration was given by ^{29}Si-NMR spectroscopy using the INEPT technique. In the case of the addition of (diphenylmethylsilyl)-dimesitylborane to phenylacetylene, the proton-decoupled ^{29}Si-NMR INEPT spectrum of **7** is shown in Fig. 5 (refocused spectrum).

This spectrum exhibited one major signal at -14.7 ppm. Unexpectedly, three other weak peaks which were not found from chromatography can be seen at -13.3, -13.1 and -10.8 ppm, respectively. So, the ^{29}Si-NMR INEPT spectroscopy revealed very sensitive in this case, whereas only very weak additional signals were detected in the ^{13}C-NMR spectrum. The highest peak at -14.7 ppm was assigned to stereoisomer **7a** and the peak at -13.3 ppm to isomer **7b**. This assignment was supported by non-decoupled ^{29}Si-NMR INEPT experiments. Thus, two different complex patterns were observed for these nuclei (Fig. 6, spectra a and b).

Qualitative analysis of each system of spins was performed thanks to the SIMEPT program (Fig. 6, spectra c and d). These results corroborated the fact that the silicon nuclei were coupled to four different ^{1}H spin systems, including the *cis* and *trans* $^3J_{Si-H_2}$ with the ethylenic H. Since $^3J_{trans}$ should be larger than $^3J_{cis}$, the ^{29}Si nuclei signal at -14.7 ppm, with the largest $^3J_{Si-H_2}$ value (16.2 Hz) was assigned to the *Z* stereoisomer **7a** [22,26]. The signal at -13.3 ppm with the smallest coupling constant (14.9 Hz) was assigned to the *E* stereoisomer **7b**. Interestingly, the efficiency of the program was confirmed by the involvement of a long-distance coupling constant $^4J_{Si-H_8} = 0.8$ Hz (Table 2). If this parameter is ignored, the simulated spectrum does not fit correctly the experimental data.

Moreover, this strategy enabled us to assign other small ^{29}Si-NMR peaks. The simulated spectrum of the signal at -10.8 ppm revealed a coupling constant J_{Si-H} of 11.7 Hz (Fig. 7). Such a value is consistent with the structure of one of the two isomers **7c** or **7d**, resulting from the reverse addition to the triple bond, i.e. $^2J_{Si-H_2}$. We can reasonably postulate that the fourth signal at -13.1 ppm corresponds to the other isomer.

From a quantitative point of view, it must be emphasised that the INEPT sequence cannot afford any direct

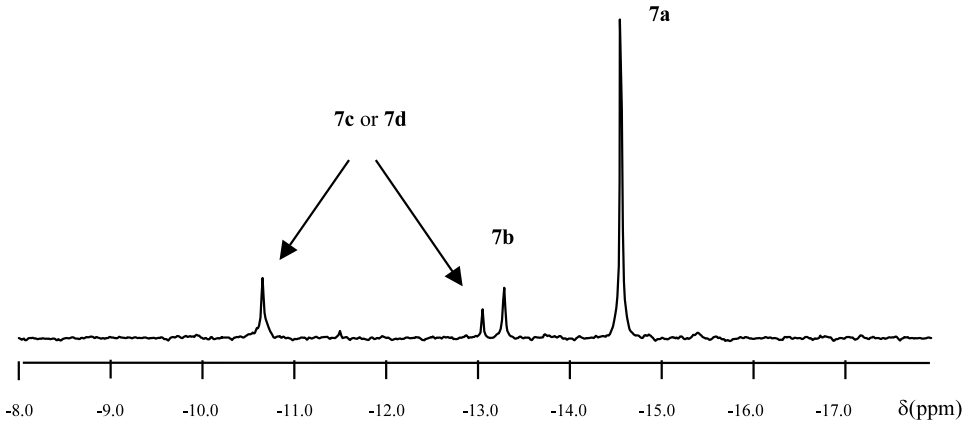

Fig. 5. Experimental ^{1}H-decoupled ^{29}Si-NMR INEPT spectrum of borosilylation product **7**.

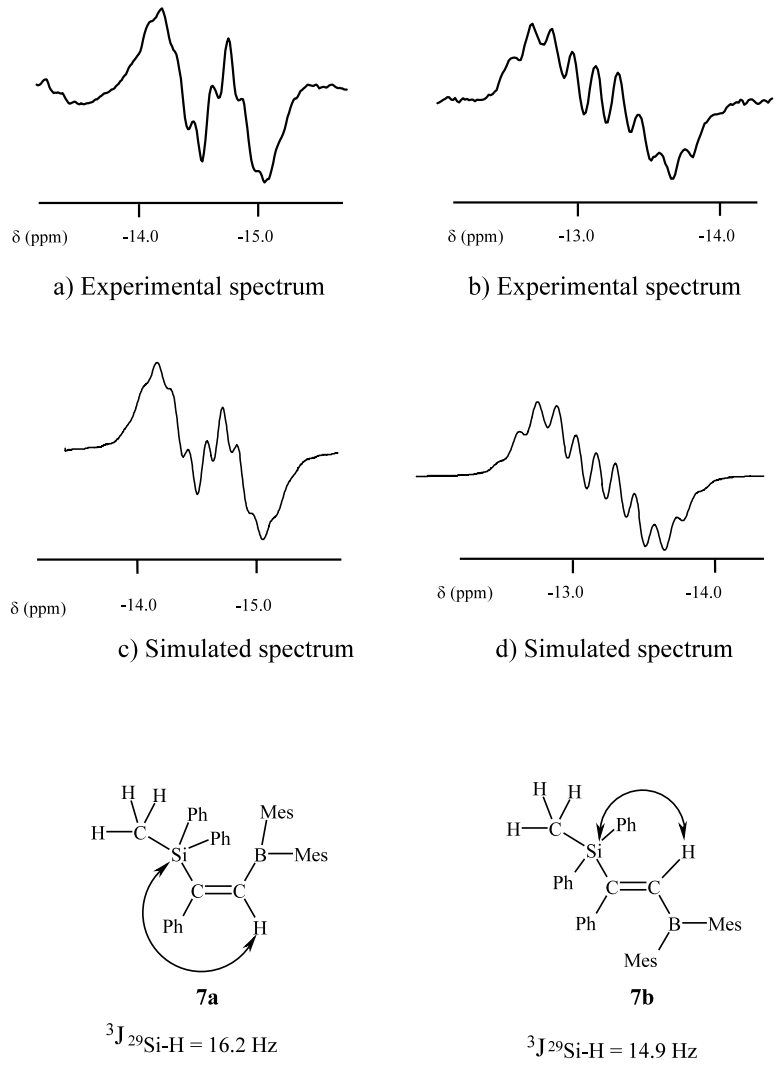

Fig. 6. Experimental and simulated ^{29}Si-NMR INEPT spectra of isomers **7a** and **7b**.

relationship between the intensities of the signals and the ratios of the geometric isomers. Indeed, the spectra resulting from INEPT sequences are tightly dependent on the parameters τ, Δ, J and multiplicity. Therefore, the quantitative determination of each isomer requires the knowledge of all the system of spins of each compound, as well as their relative response factors. In this context, the SIMEPT program has emerged as a very pertinent tool for the reconstruction of the spectra, as relative response factors can be easily calculated for every given parameter sets. The following values for the response factors were obtained: 4.7 (signal at -10.8 ppm), 2.2 (signal at -13.3 ppm) and 1 for the main signal (signal at -14.7 ppm).

In the case of the product **9**, the stereochemistry of the reaction was determined as in the case of product **7**, thanks to ^{29}Si-NMR spectroscopy. Thus, the main addition product having the largest coupling constant $^3J_{Si-H_2}$ (16.2 Hz) corresponds to the isomer *Z* **9a**.

3. Experimental

3.1. General

All manipulations were carried out under Ar atmosphere using standard vacuum techniques. Handling of air sensitive powders and solids was performed under controlled atmosphere in a glove box containing dry nitrogen. The solvents were purified by conventional means and distilled prior to use. $Pd_2(dba)_3$ was purchased from Aldrich.

The NMR spectra were recorded in C_6D_6 or $CDCl_3$ using Bruker AC 250 (^{1}H and ^{13}C) and a DPX 200 spectrometers (^{29}Si and ^{11}B). Chemical shifts are reported in ppm and are referenced to Me_4Si (^{1}H, ^{13}C, ^{29}Si) or $BF_3{\cdot}Et_2O$ (^{11}B).

2D *J*-resolved INEPT is a technique to obtain coupled spectra. However, the large value of the coupling constant $^1J_{^{13}C-^1H}$ (in the range of 140 Hz) requires a

Table 2
$J_{^{29}Si-^{1}H}$ and $J_{^{1}H-^{1}H}$ coupling constants used for the simulation of spectra in Fig. 6

Compound	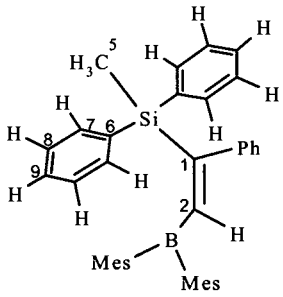	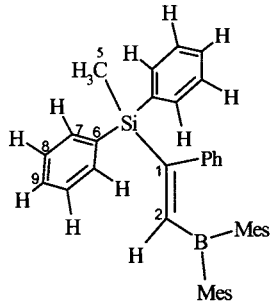
	Z isomer 7a	E isomer 7b
Coupling constants (Hz)	^{2}JSi-H$_5$ = 6.6 ^{3}JSi-H$_7$ = 5.1 ^{4}JSi-H$_8$ = 0.8 ^{3}JSi-H$_2$ = 16.2 (trans) ^{3}JH$_7$-H$_8$ = 7.7	^{2}JSi-H$_5$ = 6.6 ^{3}JSi-H$_7$ = 5.1 ^{4}JSi-H$_8$ = 0.8 ^{3}JSi-H$_2$ = 14.9 (cis) ^{3}JH$_7$-H$_8$ = 7.7

broad window in the F1 domain, thus lowering the resolution. When refocusing pulses are replaced by BIRD pulses, direct coupling ^{1}J can be suppressed. The corresponding window is narrowed, so the resolution increases [23]. The coupling constants were measured by the heteronuclear ^{1}H–^{13}C J-resolved BIRD 2D INEPT technique, in the phase sensitive mode, using the following sequence: D_1–(90°$^{1}_{x}$H)–τ–(180°$^{1}_{x}$H)(180°$^{13}_{x}$C)–τ–(90°$^{1}_{\pm y}$H)(90°$^{13}_{x}$C)–d_0 (BIRD) d_0 acquisition in TPPI mode with proton decoupling. BIRD–(90$^{\phi}_{x}$H)–d_6–(180°$^{1}_{x}$H)(180°$^{13}_{x}$C)–d_6–(90°$^{1}_{x}$H). The spectrum was recorded using spectral widths of 3550 ± 50 Hz in the F2 and F1 dimensions, respectively. A total of 32 transients were accumulated for the 256 increments of t_1. The relaxation delay D_1 was 1 s, $\tau = 0.053$ s, $d_6 = 0.00357$ s, increment = 0.0025 s.

Non-refocused INEPT spectra were simulated on a PC using the program previously described for ^{119}Sn and ^{29}Si [25]. The following parameters were used: ^{29}Si $\tau = 0.0357$ s, $\Delta = 0.02$ s; ^{13}C $\tau = 0.053$ s, $\Delta = 0.00357$ s.

IR data were collected using a Perkin–Elmer Paragon 1000 spectrometer. The samples were prepared as KBr pellets or films between KBr plates.

Mass spectra (MALDI-TOFMS) were obtained in a VG TofSpec-SE Fisons Instruments spectrometer (20 kV) from a THF solution containing the same amounts of the sample and 5-chlorosalicyclic acid as the matrix. Low and high resolution LSIMS (+) spectra were obtained in a VG Autospec-EQ (EBEQQ) spectrometer using 3-nitrobenzylic alcohol as the matrix.

Elemental analyses were performed by the Service Central d'Analyses du CNRS, BP 22, 69390 F-Vernaison.

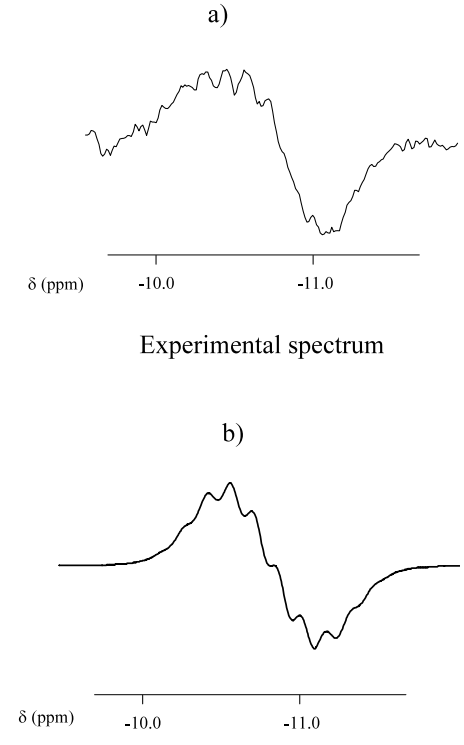

Fig. 7. Experimental and simulated ^{29}Si-NMR INEPT spectra of products **7c** or **7d**.

Melting temperatures were obtained in a Kofler hot bench or a capillary melting point apparatus.

3.2. Synthesis of organosilylboranes

Organosilyllithium reagents were obtained according to previously reported procedures [27–29]. Thus, methyldiphenylsilyllithium was prepared from finely divided lithium (0.28 g, 0.04 mol) and methyldiphenylchlorosilane (4.45 g, 0.02 mol) in THF (40 ml) at −10 °C. The mixture was degassed using ultrasounds prior to addition of the chlorosilane. Other silyllithium reagents were obtained in a similar way. Dimesitylfluoroborane (5.4 g, 0.02 mol) and dry THF (15 ml) were placed in a three-necked Pyrex® flask equipped with a magnetic bar, a pressure-equalising dropping funnel, a reflux condenser and an Ar inlet. The flask was cooled at −60 °C and magnetically stirred. Methyldiphenylsilyllithium in THF was added dropwise over 30 min and allowed to heat at room temperature under stirring over 3 h. After evaporation of the solvent, the crude solid was washed with 25 ml of petroleum ether, chiefly to eliminate the excess of Mes_2BF. The remaining solid was extracted with petroleum ether (2×150 ml) and the solution filtered under inert atmosphere to separate the lithium salts. Then, the remaining solid was washed with toluene (25 ml) and both solutions evaporated separately, yielding in each case a yellow–green powder. The product was crystallised from a petroleum ether solution. Yield: 64%.

3.3. $Pd_2(dba)_3(etpo)_2$

$Pd_2(dba)_3$ (28 mg, 0.03 mmol) and etpo (14 mg, 0.085 mmol) were introduced under Ar in a 50 ml Schlenk tube and capped with a septum. Toluene (2 ml) was added with a syringe. Then, the Schlenk flask was fitted with a condenser and refluxed for a few minutes until formation of a green colour.

3.4. Silaboration products

Organosilylborane **1** (0.447 g, 1 mmol), phenylacetylene in excess (0.0204 g, 2 mmol) and toluene (3 ml) were introduced in a round-bottom flask equipped with an Ar inlet and a magnetic bar. This solution was slowly added onto the previously prepared catalyst solution in the Schlenk tube using a syringe. After heating at 120 °C under stirring for 12 h, the solvent and phenylacetylene in excess were eliminated under vacuum. The crude product **7** was passed through a neutral alumina column under Ar using petroleum ether as the eluent.

The same procedure was used to prepare the products **8**–**10**.

3.5. Physicochemical characterisation

3.5.1. (Diphenylmethylsilyl)dimesitylborane (*1*)

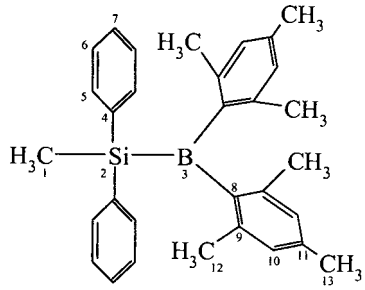

M.p. 105 °C. ^{29}Si-NMR (C_6D_6, ppm): −25.0. ^{11}B-NMR (ppm): 103.0. ^{1}H-NMR (ppm): 0.75 (s, 3H, 1), 2.08 (s, 12H, 12), 2.13 (s, 6H, 13), 6.69 (s, 4H, 10), 7.11 (m, 6H, 6, 7), 7.45 (m, 4H, 5). ^{13}C-NMR (ppm): −0.8 (1), 21.2 (13), 24.3 (12), 128.0 (6), 128.8 (7), 129.1 (10), 135.5 (5), 138.8 (9), 139.4 (11), 140 (4), 145.3 (8). Anal. calc. for $C_{31}H_{35}BSi$ (446.51): C, 83.39; H, 7.90; B, 2.42; Si, 6.29. Found: C, 82.9; H, 7.07; B, 2.40; Si, 7.05%. EIMS; m/z (%): 249.1 (100%, Mes_2B^+); 446.2 (0.5%, $MePh_2SiBMes_2^+$). MALDI TOF LD+: 511.23 (100%, $[M + Na]^+$), 527.18 (50%, $[M + K]^+$). Low resolution LSIMS: 223.1 (28%, $MePh_2SiBMe^+$); 249.1 (55%, Mes_2B^+); 264.1 (24%, $MeBMes_2^+$); 301.1 (44%, $MesPh_2Si^+$). High resolution LSIMS; $C_{31}H_{36}BSi$ ($[MePh_2SiBMes_2 + H]^+$): 447.260345 (Found); 447.267935 (Calc.).

3.5.2. (Diphenyl-tert-butylsilyl)dimesitylborane (*2*)

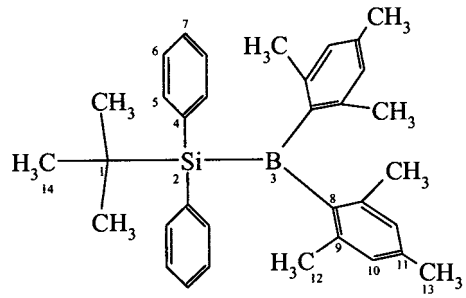

M.p. 132 °C. ^{29}Si-NMR (C_6D_6, ppm): −20.1. ^{11}B-NMR (ppm): 110.0. ^{1}H-NMR ($CDCl_3$, ppm): 1.38 (s, 9H, 14), 2.10 (s, 18H, 12, 13), 6.66 (s, 4H, 10), 7.10 (m, 6H, 6, 7), 7.75 (m, 4H, 5). ^{1}H-NMR (CD_2Cl_2, ppm): 1.28 (s, 9H, 14), 1.93 (s, 12H, 12), 2.24 (s, 6H, 13), 6.68 (s, 4H, 10), 7.15–7.23 (m, 6H, 6, 7), 7.52–7.56 (m, 4H, 5). ^{13}C-NMR (ppm): 20.6 (1), 21.0 (13), 25.1 (12), 30.2 (14), 127.7 (6), 128.4 (7), 129.1 (10), 136.6 (5), 138.0 (4), 138.9 (9), 139.2 (11), 146.4 (8). Anal. calc. for

$C_{34}H_{41}BSi$ (488.59): C, 83.58; H, 8.46; B, 2.21; Si, 5.75. Found: C, 83.25; H, 7.75; B, 2.13; Si, 5.50%. MS: MALDI TOF LD+: 511.23 (100%, $[M+Na]^+$); 527.18 (50%, $[M+K]^+$). Low resolution LSIMS: 249.2 (100%, Mes_2B^+); 301.1 (27%, $MesPh_2Si^+$).

*3.5.3. [(Z)-2-(Dimesitylboryl)-1-phenylethenyl]-(methyl)diphenylsilane (**7a**)*

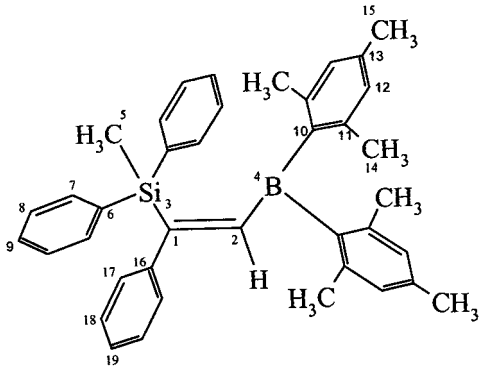

^{29}Si-NMR (ppm): −14.7. $^2J_{Si-H_5}=6.6$ Hz, $^3J_{Si-H_7}=5.1$ Hz, $^4J_{Si-H_8}=0.8$ Hz, $^3J_{H_7-H_8}=7.7$ Hz, $^3J_{Si-H_2}=16.20$ Hz. ^{11}B-NMR (ppm): 80. ^{1}H-NMR (ppm): 0.58 (s, 3H, 5), 2.15 (s, 12H, 14), 2.19 (s, 6H, 15), 6.83 (s, 4H, 12), 7.17 (m, 5H, 17, 18, 19), 7.2–7.4 (m, 10H, 7, 8, 9), 7.64 (s, 1H, 2). ^{13}C-NMR (ppm): −0.7 (5), 21.5 (15), 24.1 (14), 126.2 (17), 128.1 (8), 128.4 (18), 128.9 (9, 19), 129.0 (12), 135.4 (7), 137.0 (13), 139.5 (6), 141.1 (11), 142.7 (16), 149.8 (10), 154 (1), 161.1 (2). MS; *z*/*e* (low resolution LSIMS): 249.2 (100%, Mes_2B^+); 301.1 (17%, $MesPh_2Si^+$); 351.2 (21%, $[M-Mes-Ph-H]^+$); 429.2 (31%, $[M-Mes]^+$); 471.3 (23%, $[M-Ph]^+$); 533.3 (4%, $[M-Me]^+$); 548.3 (3%, M^+). High resolution LSIMS; $C_{39}H_{41}BSi$ $[M]^+$: 548.306930 (Found); 548.307060 (Calc.).

*3.5.4. [(E)-2-(Dimesitylboryl)-1-phenylethenyl](methyl)-diphenylsilane (**7b**)*

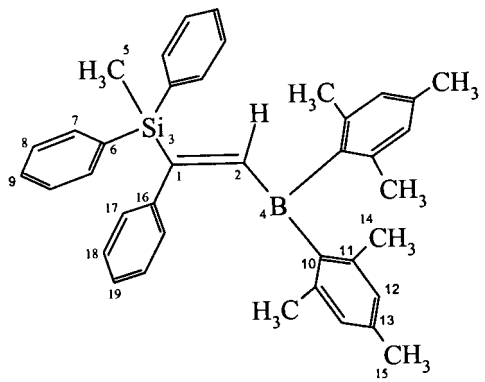

^{29}Si-NMR (ppm): −13.3. $^2J_{Si-H_5}=6.6$ Hz, $^3J_{Si-H_7}=5.1$ Hz, $^4J_{Si-H_8}=0.8$ Hz, $^3J_{H_7-H_8}=7.7$ Hz, $^3J_{Si-H_2}=14.90$ Hz.

*3.5.5. [(Z,E)-2-(Dimesitylboryl)-2-phenylethenyl]-(methyl)diphenylsilane (**7c** and **7d**)*

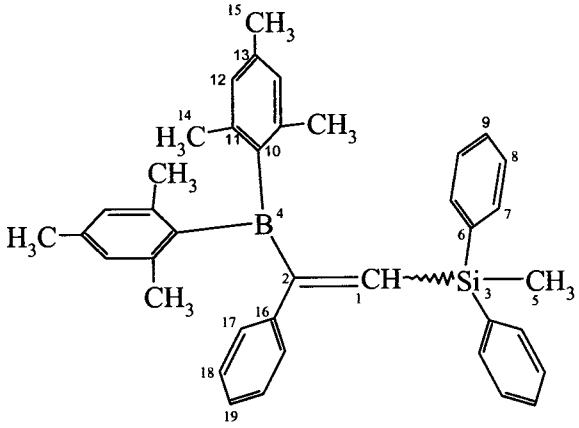

^{29}Si-NMR (ppm): −10.8, −11.5. $^2J_{Si-H_5}=6.6$ Hz, $^3J_{Si-H_7}=5.1$ Hz, $^4J_{Si-H_8}=0.8$ Hz, $^2J_{Si-H_1}=11.7$ Hz, $^3J_{H_7-H_8}=7.7$ Hz.

*3.5.6. [(Z)-2-(Dimesitylboryl)-1-pentylethenyl]-(methyl)diphenylsilane (**8a**)*

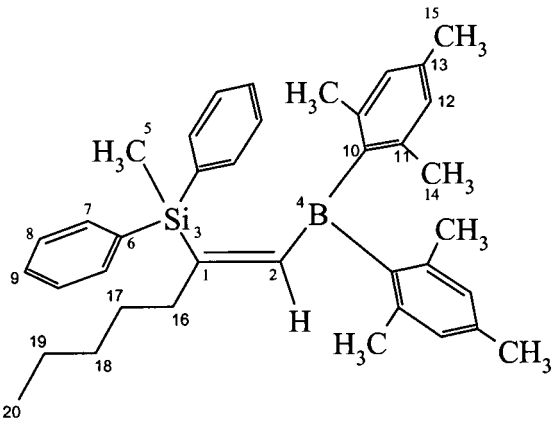

^{29}Si-NMR (ppm): −13.2. $^2J_{Si-H_5}=6.6$ Hz, $^3J_{Si-H_7}=5.1$ Hz, $^4J_{Si-H_8}=0.8$ Hz, $^3J_{Si-H_2}=16.3$ Hz, $^3J_{H_7-H_8}=7.7$ Hz. ^{11}B-NMR (ppm): 80.0. ^{1}H-NMR (ppm): 0.42 (s, 3H, 5), 0.67 (m, 3H, 20), 0.84 (m, 4H, 18, 19), 1.08 (m, 2H, 17), 2.17 (s, 6H, 15), 2.24 (s, 12H, 14), 2.41 (m, 2H, 16), 6.71 (s, 4H, 12), 7.19 (m, 6H, 8, 9), 7.51 (m, 4H, 7), 7.60 (s, 1H, 2). ^{13}C-NMR (ppm): −1.5 (5), 14.3 (20), 21.3 (15), 22.7 (19), 24.0 (14), 29.8 (17), 32.4 (18), 42.4 (16), 128.1 (8), 129.2 (12), 129.5 (8, 14), 135.4 (7), 137.6 (13), 139.1 (6), 140.9 (11), 143.6 (10), 156.3 (1), 156.9 (2). MS; *z*/*e* (low resolution LSIMS): 249.2 (100%, Mes_2B^+); 301.1 (7%, $MesPh_2Si^+$); 345.3 (15%, $[M-Mes-Ph-H]^+$); 423.2 (46%, $[M-Mes]^+$);

465,3 (32%, $[M-Ph]^+$); 527.3 (6%, $[M-Me]^+$); 541.2 (6%, $[M-H]^+$). High resolution LSIMS; $C_{29}H_{36}BSi$ ($[M-Mes]^+$): 423.266218 (Found); 423.267935 (Calc.)

*3.5.7. [(Z)-2-(Dimesitylboryl)-1-phenylethenyl]-(tert-butyl)diphenylsilane (**9a**)*

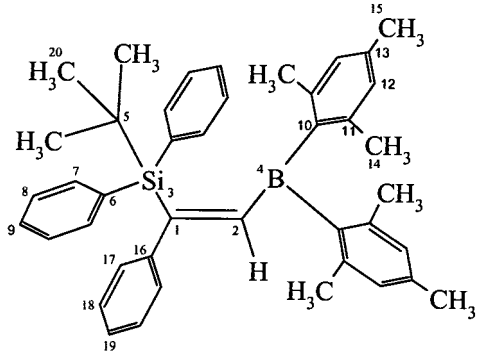

^{29}Si-NMR (ppm): −7.1. $^2J_{Si-H_5} = 6.6$ Hz, $^3J_{Si-H_7} = 5.1$ Hz, $^4J_{Si-H_8} = 0.8$ Hz, $^3J_{H_7-H_8} = 7.7$ Hz, $^3J_{Si-H_2} = 16.2$ Hz. ^{11}B-NMR (ppm): 88.0. ^{1}H-NMR (ppm): 0.97 (s, 9H, 20), 2.1 (s, 12H, 14), 2.37 (s, 6H, 15), 6.78 (s, 4 H, 12), 7.1–7.4 (m, 15H, 7, 8, 9, 17, 18, 19), 7.64 (s, 1H, 2). ^{13}C-NMR (ppm): 20.0 (5), 21.2 (15), 24.3 (14), 29.7 (20), 126.3 (17), 127.3 (8), 127.9 (9, 19), 128.4 (18), 128.5 (12), 135.0 (13), 137.3 (7), 138.7 (6), 140.7 (11), 143.0 (16), 145.0 (10), 150.6 (1), 165.0 (2). MS; *z*/*e* (low resolution LSIMS): 239.0 (17%, *tert*-$BuPh_2Si^+$); 249.2 (100%, Mes_2B^+); 301.1 (57%, $MesPh_2Si^+$); 325.1 (9%, $[MesPh_2SiH]Na^+$); 471.2 (32%, $[M-Mes]^+$); 513.2 (16%, $[M-Ph]^+$); 533.3 (81%, $[M-tert\text{-}Bu]^+$); 575.3 (1%, $[M-Me]^+$); 589.3 (5%, $[M-H]^+$); 613.2 (2%, $[M+Na]^+$). High resolution LSIMS; $C_{38}H_{38}BSi$ ($[M-tert\text{-}Bu]^+$): 533.284410 (Found); 533.283585 (Calc.).

*3.5.8. [(Z)-2-(Dimesitylboryl)-1-pentylethenyl]-(tert-butyl)diphenylsilane (**10a**)*

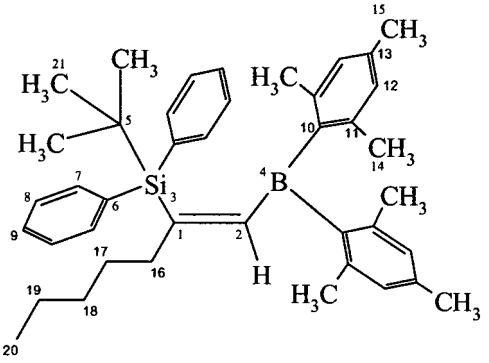

^{29}Si-NMR (ppm): −5.4. $^3J_{C_5-H_{21}} = -3.3$ Hz. ^{11}B-NMR (ppm): 75.0. ^{1}H-NMR (ppm): 0.82 (m, 3H, 20), 1.2 (m, 4H, 18, 19), 1.25 (s, 9H, 21), 1.67 (m, 2H, 17), 2.09 (s, 12H, 14), 2.14 (s, 6H, 15), 2.47 (m, 2H, 16), 6.63 (s, 4H, 12), 7.04–7.17 (m, 6H, 8, 9), 7.51 (m, 4H, 7), 7.62 (s, 1H, 2). ^{13}C-NMR (ppm): 14.4 (20), 19.9 (5), 21.2 (15), 23.0 (19), 24.3 (14), 29.0 (17), 30.3 (21), 32.5 (18), 40.7 (16), 127.7 (8), 128.4 (12), 129.3 (9), 135.2 (13), 137.2 (7), 138.7 (6), 140.8 (11), 143.0 (10), 145.5 (1), 158.1 (2). MS; *z*/*e* (low resolution LSIMS): 239.0 (14%, *tert*-$BuPh_2Si^+$); 249.2 (100%, Mes_2B^+); 301.1 (13%, $MesPh_2Si^+$); 465.3 (37%, $[M-Mes]^+$); 507.3 (19%, $[M-Ph]^+$); 527.3 (80%, $[M-tert\text{-}Bu]^+$); 569.3 (1%, $[M-Me]^+$); 583.3 (4%, $[M-H]^+$); 607.3 (2%, $[M+Na]^+$); 623.5 (1%, $[M+K]^+$). High resolution LSIMS; $C_{37}H_{44}BSi$ ($[M-tert\text{-}Bu]^+$): 527.328803 (Found); 527.330535 (Calc.).

4. Conclusions

Novel stable organosilylboranes bearing dimesitylboryl groups were synthesised. In spite of their steric hindrance, they give addition products with terminal acetylenic hydrocarbons in the presence of $Pd_2(dba)_3(etpo)_2$ complex as the catalyst. The reaction took place smoothly regio- and stereoselectively, giving one major isomer in good yields. Thus, the dimesitylboryl group added to the terminal carbon and the organosilyl group to the internal, according to a *syn*-addition. The structures of the products were unambiguously demonstrated, thanks to ^{13}C- and ^{29}Si-NMR spectroscopy using various INEPT techniques. These results are in good agreement with those previously reported for the silaboration using silylpinacolboranes and silyldiaminoboranes.

Acknowledgements

The authors thank the Conseil Regional d'Aquitaine (CRA) for financial support.

References

[1] A.H. Cowley, H.H. Sisler, G.E. Ryschkewitsch, J. Am. Chem. Soc. 82 (1960) 501.
[2] D. Seyferth, H.P. Kogler, J. Inorg. Nucl. Chem. 15 (1960) 99.
[3] H. Nöth, G. Höllerer, Angew. Chem. 74 (1962) 718.
[4] H. Nöth, G. Höllerer, Chem. Ber. 99 (1966) 2197.
[5] W. Biffar, H. Nöth, Chem. Ber. 115 (1982) 934.
[6] See for example: (a) B. Pachaly, R. West, Angew. Chem. Int. Ed. Engl. 23 (1984) 454;
(b) M. Haase, U. Klingebiel, Angew. Chem. Int. Ed. Engl. 24 (1985) 324.
[7] J.D. Buynak, B. Geng, Organometallics 14 (1995) 3112.
[8] M. Suginome, T. Matsuda, Y. Ito, Organometallics 19 (2000) 4647.
[9] M. Suginome, H. Nakamura, Y. Ito, Angew. Chem. Int. Ed. Engl. 36 (1997) 2516.

[10] M. Suginome, T. Matsuda, Y. Ito, Organometallics 17 (1998) 5233.
[11] M. Suginome, H. Nakamura, Y. Ito, Chem. Commun. (1996) 2777.
[12] M. Suginome, T. Matsuda, Y. Ito, Tetrahedron 55 (1999) 8787.
[13] S.-y. Onosawa, Y. Hatanaka, M. Tanaka, Chem. Commun. (1997) 1229.
[14] M. Suginome, T. Matsuda, Y. Ito, J. Am. Chem. Soc. 122 (2000) 11015.
[15] M. Suginome, Y. Ohmori, Y. Ito, J. Organomet. Chem. 611 (2000) 403.
[16] J.-P. Pillot, M. Birot, E. Bonnefon, J. Dunoguès, J.-C. Rayez, M.-T. Rayez, D. Liotard, J.-P. Desvergne, Chem. Commun. (1997) 1535.
[17] E. Bonnefon, M. Birot, J. Dunoguès, J.-P. Pillot, C. Courseille, F. Taulelle, Main Group Met. Chem. 19 (1996) 761.
[18] W. Biffar, H. Nöth, H. Pommerenning, Angew. Chem. Int. Ed. Engl. 19 (1980) 56.
[19] S.-y. Onozawa, Y. Hatanaka, T. Sakakura, S. Shimada, M. Tanaka, Organometallics 15 (1996) 5450.
[20] N.M.D. Brown, F. Davidson, J.W. Wilson, J. Organomet. Chem. 209 (1981) 11.
[21] M. Lequan, R.M. Lequan, K.C. Ching, M. Barzoukas, A. Fort, G. Lahoucine, G. Bravic, D. Chasseau, J. Gaultier, J. Mater. Chem. 2 (1992) 719.
[22] E. Liepins, I. Birgele, E. Lukevics, V.D. Sheludyakov, V.G. Lahtin, J. Organomet. Chem. 385 (1990) 185.
[23] D.M. Thomas, M.R. Bendall, D.T. Pegg, D.M. Doddrell, J. Field, J. Magn. Res. 42 (1981) 298.
[24] M. Harket, B. De Jéso, J.-C. Lartigue, M. Pétraud, M. Ratier, Carbohydrate Res. 263 (1994) 155.
[25] J.-C. Lartigue, M. Pétraud, M. Harket, B. De Jéso, M. Ratier, Comput. Chem. 20 (1996) 219.
[26] M. Haake, J. Natterer, J. Bargon, J. Am. Chem. Soc. 118 (1996) 8688.
[27] H. Gillman, G.E. Dunn, J. Am. Chem. Soc. 73 (1951) 1951.
[28] For a review on the preparation of silyllithium compounds, see for example: A. Kawachi, K. Tamao, Bull. Chem. Soc. Jpn. 70 (1997) 945.
[29] H.C. Brown, V.H. Dodson, J. Am. Chem. Soc. 79 (1957) 2302.